# Advanced Characterisation of Pore Structure in Next-Generation Reactor Graphites

Bradley Moresby-White[a], Katie L. Jones[a,*], G. Peter Matthews[a], Giuliano M. Laudone[a]

[a]*Faculty of Science and Engineering, University of Plymouth, Plymouth, UK*

---

**Abstract**

Nuclear grade graphite

*Keywords:* keyword, keyword, keyword

---

## 1. Introduction

This is a citation.[1]

## 2. Methodology

### 2.1. Materials

Virgin graphite samples of two grades, IG-110 and IG-430, were supplied by Toyo Tanso Ltd™, Osaka, Japan. The properties of both grades are tabulated (Table 1).

IG-110 is currently employed in the three existing HTGRs worldwide, while IG-430 is designed to deliver increased density, strength, and thermal conductivity for future applications.[3] (Table 1). Both grades comply with *ASTMD7219-19*, including the requirement for a minimum bulk density exceeding 1.7 g/cm$^3$ [4] (Table 1).

### 2.2. Sample preparation

The cuboids were sub-sampled from the virgin graphite blocks, with dimensions of approximately 10 mm x 10 mm x 100 mm. The sub-samples were further subsampled into cuobids of side lengths 7mm, providing 3 cuboids per grade. Samples were polished via SiC polishing pads up to a grit size of P5000, to minimise topographical variations induced by sample preparation that could scatter the electron beam during SEM, potentially causing artifacts [5].Samples were sonicated in 2-propanol for 24h to remove any contaminants introduced by the lubricant used in the machining process. The samples were then dried under vacuum for 12 h at 305±5 °C using the BELPREP-vac (MicrotracBEL, Japan) in order to remove any residual moisture introduced during the sonication process.

### 2.3. Micrograph generation

The JEOL™IT510 Scanning Electron Microscope was used in the generation of the contiguous set of individual micrographs from which the full composite is assembled. The *Image Montage* capability, within the JEOLInScope™package, performed this function. The system captures a set number of micrographs, with the motorised stage moving the electron beam over the specified area with a set overlap, with the software adjusting stigmation, contrast, and brightness. Shifts in contrast and brightness were on the order of 1% and thus negligible in affecting the final thresholded image, particularly following fusion. The parameters selected are tabulated (Table 2).

Make sure to double check that figure for ACB

### 2.4. Composite assembly

The composite assembly (i.e., "stitching") stage has a significant impact on the porosity values derived from the final composite, as incorrect fusion will misrepresent pore structures. A stitching method based on the phase correlation approach originally developed by **(author?)** [6], amongst the most popular and well-tested approaches available for image registration, was selected and operated as a plug-in within ImageJ/Fiji [7]. This method

*Corresponding author.

*Email address:* `katie.jones@plymouth.ac.uk` (Katie L. Jones)

Table 1: Manufacturer's characterisation of the graphite types [2]

| Grade | Coke source | Bulk density/g $cm^3$ | Filler particle size/$\mu$m) | Tensile strength/MPa | Young's modulus/GPa | Thermal conductivity/W $m^{-1}K^{-1}$ |
|---|---|---|---|---|---|---|
| IG-110 | Petrol | 1.77 | 10 | 25 | 9.8 | 120 |
| IG-430 | Pitch | 1.82 | 10 | 37 | 10.8 | 140 |

represents a development of the original phase correlation method, and was selected for its solid mathematical foundations[7].

The mathematics of phase correlation methods is further detailed in the Appendix. In this work, the primary advantage is the application of a smooth, non-linear intensity transition between the overlapping micrographs. This is a prerequisite as the selection of an intensity threshold is not possible if the variations in contrast and brightness between micrographs are non-trivial. Additionally, this method also avoids the propagation of errors by consecutive registration steps, which is key at this scale [7]. Another benefit is the subpixel accuracy of the fusion, as incorrect alignments would generate false pore diameters. Finally, the method is computationally efficient, which is important where the input micrographs sum to several hundred megabytes in size.

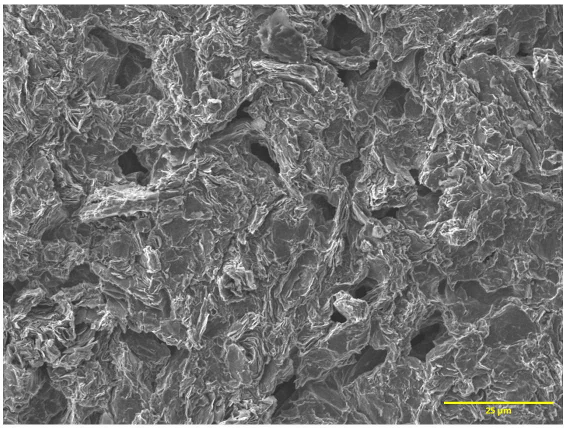


Figure 1: PLACEHOLDER

Table 2: Parameters for composite assembly captured with the JEOL IT510 SEM using Image Montage Mode

| Parameters | Values |
|---|---|
| Magnification (X) | 1000 |
| Resolution ($\mu$m/px) | 0.1 |
| Surface area per micrograph ($\mu m^2$) | 12 288 |
| Overlap (%) | 10 |
| Micrographs per sample (n) | 196 |

## References


[1] K. L. Jones, G. P. Matthews, G. M. Laudone, The effect of irradiation and radiolytic oxidation on the porous space of gilsocarbon nuclear graphite measured with mercury porosimetry and helium pycnometry, Carbon 158 (2020) 256–266. doi:https://doi.org/10.1016/j.carbon.2019.11.084. URL https://www.sciencedirect.com/science/article/pii/S0008622319312175

[2] K. Jones, G. Laudone, G. Matthews, A multi-technique experimental and modelling study of the porous structure of ig-110 and ig-430 nuclear graphite, Carbon 128 (2018) 1–11. doi:10.1016/j.carbon.2017.11.076.

[3] Toyo Tanso Co., Ltd., Atomic power and nuclear fusion, accessed April 21, 2025 (2025). URL https://www.toyotanso.com/us/en/Products/application/atomic-nuclear.html

[4] ASTM International, D7219-19 Standard Specification for Isotropic and Near-isotropic Nuclear Graphites, published August 2019; supersedes D7219-08R14 (2019).

[5] N. Fang, R. Birch, T. Britton, Optimizing broad ion beam polishing of zircaloy-4 for electron backscatter diffraction analysis, Micron 159 (2022) 103268. doi:10.1016/j.micron.2022.103268.

[6] C. D. Kuglin, D. C. Hines, The phase correlation image alignment method, in: Proceedings of the International Conference on Cybernetics and Society, 1975, pp. 163–165.

[7] S. Preibisch, S. Saalfeld, P. Tomancak, Globally optimal stitching of tiled 3d microscopic image acquisitions, Bioinformatics 25 (11) (2009) 1463–1465. arXiv:2009 Apr 3, doi:10.1093/bioinformatics/btp184.